Complex vibration of pulsatile fluid-conveying ultrasmall tubes embedded in a nonlinear elastic medium

Mergen H. Ghayesh (1), Ali Farajpour (1) and Hamed Farokhi (2)

(1) School of Mechanical Engineering, University of Adelaide, South Australia 5005, Australia
(2) Department of Mechanical and Construction Engineering, Northumbria University, Newcastle upon Tyne NE1 8ST, UK

ABSTRACT

In the present paper, the role of the flow pulsation in the scale-dependent complex vibration of ultrasmall tubes under the action of an axial pretention is investigated. The main focus of the present study is on the chaotic vibration response of the ultrasmall system. The effect of the internal energy friction is also considered via help of the Kelvin-Voigt model. In practical applications, tubes and pipes are usually surrounded by an elastic foundation. Therefore, in the current study, it is assumed that the ultrasmall tube is embedded in a nonlinear elastic medium. The theory of couple stress as well as the theory of an Euler-Bernoulli beam are utilised to develop a modified scale-dependent model. An energy/work principle is also utilised for the derivation of the energy potential, motion energy and the external work as well as the equations of motions. Employing Galerkin's procedure gives the discretised version of the differential equations of the pulsatile fluid-conveying ultrasmall tube embedded in a nonlinear elastic foundation. Finally, application of a time-integration scheme gives the nonlinear characteristics of the complex vibration. It is found that the flow pulsation has a significant role in the complex vibrations of ultrasmall tubes in the super critical regime. Various types of transverse motions are found depending on the amplitude of flow pulsation.

1 INTRODUCTION

In ultrasmall fluid-conveying systems such as microfluidics- and nanofluidics-based devices (Warkiani et al. 2014), solid structures such as microscale/nanoscale tubes and plates interact with the fluid part. In practical situations, the velocity of the flowing fluid can change over time. In addition, the mixing of microfluid flows is troublesome as at microscale levels, Reynolds numbers are often low. It has recently been reported that creating pulsatile fluid flows is one way of mixing microfluid flows (Cheaib et al. 2016). The source of the pulsatile fluid flow at microscale levels can be a micropump or the nature of the microfluid flow itself. Taking into account this flow pulsation is important to better these systems since it can affect mechanical characteristics. Due to the fact that the mechanical behaviour of ultrasmall structures is size-dependent, modified continuum models have been introduced in the literature by amending the classical continuum mechanics (Şimşek 2010, Aydogdu 2015, Murmu, Adhikari, and Wang 2011, Ke et al. 2012, Hadi, Nejad, and Hosseini 2018, Farajpour et al. 2018). In the present analysis, the modified couple stress theory (MCST) is employed as the modified continuum model.

In recent years, modified continuum models have been utilised in order to study the mechanics of fluid-conveying ultrasmall tubes. Wang (Wang 2010) examined the linear vibrational response of ultrasmall tubes conveying fluid flow with a constant velocity using the MCST. Kural and Özkaya (Kural and Özkaya 2017) also analysed the vibrational response of ultrasmall fluid-conveying pipes surrounded by a linear elastic medium; they explored the influence of the elastic medium on the vibrational response. In addition, in a study done by Hosseini and Bahaadini (Hosseini and Bahaadini 2016), a modified continuum model was proposed for the instability analysis of cantilever microtubes conveying fluid based on a strain gradient theory. The nonlinear vibrational response of fluid-conveying tubes at microscales was also investigated by Dehrouyeh-Semnani et al. (Dehrouyeh-Semnani, Nikkhah-Bahrami, and Yazdi 2017) via a modified couple stress model. In addition to microscale pipes conveying fluid, the mechanical characteristics of fluid-conveying nanoscale tubes have been also examined by developing nonlocal continuum models (Bahaadini and Hosseini 2016, Ansari et al. 2016, Liu, Lv, and Li 2017). The influence of a geometrical imperfection on the nonlinear buckling of microscale fluid-conveying pipes was examined by Dehrouyeh-Semnani et al. (Dehrouyeh-Semnani, Nikkhah-Bahrami, and Yazdi 2017). Furthermore, Tang et al. (Tang et al. 2014) applied the MCST, as a size-dependent theory, to curved tubes containing fluid flow at microscales; they found that the vibration characteristics of curved microtubes are substantially different from those of straight ones. The mechanical behaviour of nonlocal strain gradient pipes conveying fluid (Li et al. 2016) and the vibration of piezoelectric inhomogeneous micropipes conveying fluid (Hosseini, Maryam, and Bahaadini 2017) have been recently studied using modified continuum models.

In all of the studies mentioned above, the fluid velocity is assumed to be constant. Nonetheless, in practical situations, the speed of the flowing fluid can change over time. In this study, the influence of the flow pulsation on the size-dependent complex vibrational response of ultrasmall tubes subject to an axial pretention is analysed. The emphasis is placed on the chaotic vibration response of the ultrasmall tube. The MCST is utilised to capture size effects on the chaotic vibration response. Moreover, the influence of the internal energy friction is captured via the Kelvin-Voigt model. The ultrasmall tube is surrounded by a nonlinear elastic medium. An energy/work principle is employed to derive the governing differential equations of the ultrasmall tube. The influences of the amplitude of the fluid velocity as well as the mean value of the fluid velocity on the size-dependent complex vibration are discussed.

2 SIZE-DEPENDENT NONLINEAR MODELLING

A viscoelastic tube conveying pulsatile flow at ultrasmall levels is shown in Fig. 1. The viscoelastic tube is resting on a nonlinear elastic medium. The ultrasmall tube is of cross-sectional area A, length L, internal radius R_i, and external radius R_o. The nonlinear elastic medium is characterised by k_1 (the linear stiffness coefficient) and k_2 (the nonlinear stiffness coefficient). An axial pretention denoted by T_0 is also applied to the ultrasmall tube. The Young modulus, the viscosity constant and Poisson's ratio of the tube are denoted by E, c_{vis} and ν, respectively. Moreover, in the present formulation, l denotes the scale parameter.

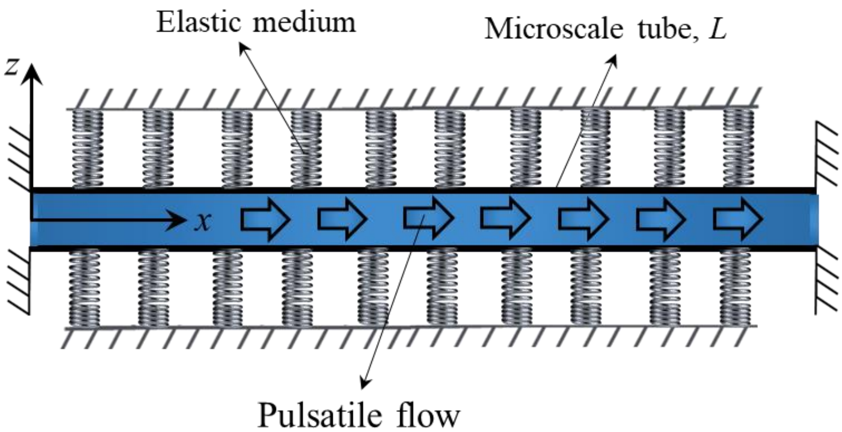

Figure 1: An ultrasmall tube conveying pulsatile flow resting on an elastic medium.

Using the Kelvin-Voigt theory, the stress-strain equation of ultrasmall tubes can be written as

$$\sigma_{xx} = \sigma_{xx(el)} + \sigma_{xx(vis)} = E\varepsilon_{xx} + c_{vis}\frac{\partial \varepsilon_{xx}}{\partial t}, \tag{1}$$

where σ_{xx}, $\sigma_{xx(el)}$, $\sigma_{xx(vis)}$ and ε_{xx} represent the axial stress, the elastic stress, the viscoelastic stress and the strain, respectively (Wang 2010, Farajpour et al., 2018). The axial strain of the ultrasmall tube is expressed as

$$\varepsilon_{xx}(x,z,t) = \sqrt{\left(1+\frac{\partial u(x,t)}{\partial x}\right)^2 + \left(\frac{\partial v(x,t)}{\partial x}\right)^2} - 1 - z\frac{\partial \theta(x,t)}{\partial x}, \tag{2}$$

in which u, v and θ denote the axial mid-plane displacement, the transverse mid-plane displacement and the cross-section rotation of the tube. In a similar way, one can write the deviatoric couple stresses (m_{ij}) as follows

$$\begin{aligned} m_{xy} &= m_{xy(el)} + m_{xy(vis)} = \tilde{E}\chi_{xy} + \tilde{c}_{vis}\frac{\partial \chi_{xy}}{\partial t}, \\ m_{yz} &= m_{yz(el)} + m_{yz(vis)} = \tilde{E}\chi_{yz} + \tilde{c}_{vis}\frac{\partial \chi_{yz}}{\partial t}, \end{aligned} \tag{3}$$

in which $\tilde{E}=El^2/(1+\nu)$ and $\tilde{c}_{vis}=c_{vis}l^2/(1+\nu)$. In Eq. (3), $m_{ij(el)}$ and $m_{ij(vis)}$ stand for the elastic and viscous parts of m_{ij}, respectively. Moreover, χ_{xy} and χ_{yz} are symmetric rotation gradient components determined as

$$\chi_{xy}=-\frac{1}{4}\frac{\partial}{\partial x}\left(\sin\theta+\frac{\partial v}{\partial x}+z\frac{\partial\cos\theta}{\partial x}\right),$$
$$\chi_{yz}=-\frac{1}{4}\frac{\partial\cos\theta}{\partial x}. \tag{4}$$

The energy/work principle can be written as

$$\int_{t_1}^{t_2}\left(\delta T_{ke}-\delta U_{pe}-\delta U_{sp}+\delta W_{vis}\right)\mathrm{d}t=0. \tag{5}$$

Here T_{ke}, U_{pe}, U_{sp} and W_{vis} stand for the kinetic energy, the potential energy, the elastic energy of the elastic medium and the work performed by viscoelastic stresses, respectively. The fluid velocity is assumed as

$$U=U_0+U_1\cos\left(\omega_f t\right), \tag{6}$$

where ω_f, U_0 and U_f are the pulsation frequency, the mean and amplitude of the fluid velocity, respectively. For developing a numerical solution, the following dimensionless parameters are employed

$$\alpha=\frac{x}{L},\ \langle\zeta,\eta,\gamma\rangle=\frac{1}{2R_o}\langle u,v,L\rangle,\ \tau=\varphi t,\ \varphi=\frac{1}{L^2}\left(\frac{EI}{M+m}\right)^{\frac{1}{2}},\ \bar{c}_{vis}=\frac{c_{vis}}{\varphi E},$$
$$\Xi_g=\frac{AL^2}{I},\ \bar{\mu}=\frac{Al^2}{2(1+\nu)I},\ \varpi_f=\frac{1}{\varphi}\omega_f,\ \Xi=L\sqrt{\frac{M}{EI}},\ \beta=\frac{M}{M+m},\ \Gamma=\frac{T_0L^2}{EI}, \tag{7}$$
$$u_f=\Xi U,\ u_{f0}=\Xi U_0,\ u_{f1}=\Xi U_1,\ \langle K_1,K_2\rangle=\frac{L^4}{EI}\langle k_1,4k_2R_o^2\rangle.$$

Here M, m and I stand for the mass per unit length of the fluid, the mass per unit length of the tube and the cross-sectional moment of inertia, respectively. Let us assume that both ends of the ultrasmall tube are clamped. These end conditions are assumed as in practical situations, especially in microfluidics-based devices, ultrasmall tubes are usually fixed at their ends. Using Galerkin's approach, the displacement components are as follows

$$\begin{Bmatrix}\zeta(\alpha,\tau)\\ \eta(\alpha,\tau)\end{Bmatrix}=\begin{Bmatrix}\sum_{l=1}^{N_x}r_l(\tau)\Phi_l(\alpha)\\ \sum_{l=1}^{N_y}q_l(\tau)\Psi_l(\alpha)\end{Bmatrix}, \tag{8}$$

where (Ψ_l, Φ_l) and (q_m, r_m) represent the shape functions and generalised coordinates, respectively. Formulating energy and work terms in Eq. (5), and then applying Eqs. (6)-(8), the discretised governing equations of the ultrasmall tube are derived. For the transverse motion, one obtains

$$\sum_{j=1}^{N_v}J_{ij}^{(1)}\ddot{q}_j-\sqrt{\beta}\varpi_f u_{f1}\sin\left(\varpi_f\tau\right)\sum_{j=1}^{N_v}J_{ij}^{(2)}q_j+\left[u_{f0}+u_{f1}\cos\left(\varpi_f\tau\right)\right]^2\sum_{j=1}^{N_v}J_{ij}^{(3)}q_j$$
$$-\Gamma\sum_{j=1}^{N_v}J_{ij}^{(4)}q_j+2\sqrt{\beta}\left[u_{f0}+u_{f1}\cos\left(\varpi_f\tau\right)\right]\sum_{j=1}^{N_v}J_{ij}^{(5)}\dot{q}_j+\left(1+\bar{\mu}\right)\sum_{j=1}^{N_v}J_{ij}^{(6)}q_j$$
$$-\frac{\Xi_g}{\gamma}\left[\frac{3}{2\gamma}\sum_{j=1}^{N_v}\sum_{k=1}^{N_v}\sum_{l=1}^{N_v}J_{ijkl}^{(7)}q_kq_jq_l+\sum_{j=1}^{N_u}\sum_{k=1}^{N_v}J_{ijk}^{(8)}r_jq_k\right]$$
$$+K_1\sum_{j=1}^{N_v}J_{ij}^{(9)}q_j+K_2\sum_{j=1}^{N_v}\sum_{k=1}^{N_v}\sum_{l=1}^{N_v}J_{ijkl}^{(10)}q_jq_kq_l-\frac{1}{\gamma}\left[\sum_{j=1}^{N_u}\sum_{k=1}^{N_v}J_{ijk}^{(11)}r_jq_k+\frac{1}{\gamma}\sum_{j=1}^{N_v}\sum_{k=1}^{N_v}\sum_{l=1}^{N_v}J_{ijkl}^{(12)}q_jq_kq_l\right]$$

$$
\begin{aligned}
&-\frac{\bar{\mu}}{4\gamma}\left[\sum_{j=1}^{N_u}\sum_{k=1}^{N_v}J_{ijk}^{(13)}r_jq_k+\frac{1}{\gamma}\sum_{j=1}^{N_v}\sum_{k=1}^{N_v}\sum_{l=1}^{N_v}J_{ijkl}^{(14)}q_jq_kq_l\right]-\frac{1}{4}\frac{\bar{\mu}}{\Xi_g\gamma^2}\sum_{j=1}^{N_v}\sum_{k=1}^{N_v}\sum_{l=1}^{N_v}J_{ijkl}^{(15)}q_jq_kq_l\\
&-\frac{\bar{c}_{vis}\Xi_g}{\gamma}\left[\frac{1}{\gamma}\sum_{j=1}^{N_v}\sum_{k=1}^{N_v}\sum_{l=1}^{N_v}J_{ijkl}^{(16)}\left(2q_j\dot{q}_kq_l+q_jq_k\dot{q}_l\right)+\sum_{j=1}^{N_u}\sum_{k=1}^{N_v}J_{ijk}^{(17)}\dot{r}_jq_k\right]\\
&+\bar{c}_{vis}\left(1+\bar{\mu}\right)\sum_{j=1}^{N_v}J_{ij}^{(18)}\dot{q}_j-\frac{\bar{c}_{vis}}{\gamma}\left[\sum_{j=1}^{N_u}\sum_{k=1}^{N_v}J_{ijk}^{(19)}\left(\dot{r}_jq_k+r_j\dot{q}_k\right)\right.\\
&+\sum_{j=1}^{N_u}\sum_{k=1}^{N_v}J_{ijk}^{(20)}\left(3\dot{r}_jq_k+4r_j\dot{q}_k\right)+\sum_{j=1}^{N_u}\sum_{k=1}^{N_v}J_{ijk}^{(21)}\left(\dot{r}_jq_k+2r_j\dot{q}_k\right)\\
&+\frac{1}{\gamma}\sum_{j=1}^{N_v}\sum_{k=1}^{N_v}\sum_{l=1}^{N_v}J_{ijkl}^{(22)}\left(6\dot{q}_jq_kq_l+6q_j\dot{q}_kq_l+8q_jq_k\dot{q}_l\right)\\
&\left.+\frac{2}{\gamma}\sum_{j=1}^{N_v}\sum_{k=1}^{N_v}\sum_{l=1}^{N_v}J_{ijkl}^{(23)}\left(\dot{q}_jq_kq_l+q_jq_k\dot{q}_l\right)+\frac{6}{\gamma}\sum_{j=1}^{N_v}\sum_{k=1}^{N_v}\sum_{l=1}^{N_v}J_{ijkl}^{(24)}q_jq_k\dot{q}_l\right]\\
&-\frac{\bar{\mu}\bar{c}_{vis}}{4\gamma}\left[\sum_{j=1}^{N_u}\sum_{k=1}^{N_v}J_{ijk}^{(25)}\left(q_k\dot{r}_j+r_j\dot{q}_k\right)+\sum_{j=1}^{N_u}\sum_{k=1}^{N_v}J_{ijk}^{(26)}\left(6\dot{r}_jq_k+8r_j\dot{q}_k\right)+\sum_{j=1}^{N_u}\sum_{k=1}^{N_v}J_{ijk}^{(27)}\left(2\dot{r}_jq_k+4r_j\dot{q}_k\right)\right.\\
&+\frac{1}{\gamma}\sum_{j=1}^{N_v}\sum_{k=1}^{N_v}\sum_{l=1}^{N_v}J_{ijkl}^{(28)}\left(17\dot{q}_jq_kq_l+15q_j\dot{q}_kq_l+20q_jq_k\dot{q}_l\right)+\\
&\left.\frac{5}{\gamma}\sum_{j=1}^{N_v}\sum_{k=1}^{N_v}\sum_{l=1}^{N_v}J_{ijkl}^{(29)}\left(\dot{q}_jq_kq_l+q_jq_k\dot{q}_l\right)+\frac{16}{\gamma}\sum_{j=1}^{N_v}\sum_{k=1}^{N_v}\sum_{l=1}^{N_v}J_{ijkl}^{(30)}q_jq_k\dot{q}_l\right]\\
&-\frac{\bar{\mu}\bar{c}_{vis}}{4\Xi_g\gamma^2}\left[\sum_{j=1}^{N_v}\sum_{k=1}^{N_v}\sum_{l=1}^{N_v}J_{ijkl}^{(31)}\left(\dot{q}_jq_kq_l+5q_j\dot{q}_kq_l+6q_jq_k\dot{q}_l\right)\right.\\
&+\sum_{j=1}^{N_v}\sum_{k=1}^{N_v}\sum_{l=1}^{N_v}J_{ijkl}^{(32)}\left(q_j\dot{q}_kq_l+q_jq_k\dot{q}_l\right)+6\sum_{j=1}^{N_v}\sum_{k=1}^{N_v}\sum_{l=1}^{N_v}J_{ijkl}^{(33)}q_jq_k\dot{q}_l\\
&+4\sum_{j=1}^{N_v}\sum_{k=1}^{N_v}\sum_{l=1}^{N_v}J_{ijkl}^{(34)}\left(q_j\dot{q}_kq_l+q_jq_k\dot{q}_l\right)\\
&\left.+10\sum_{j=1}^{N_v}\sum_{k=1}^{N_v}\sum_{l=1}^{N_v}J_{ijkl}^{(35)}\left(q_j\dot{q}_kq_l+q_jq_k\dot{q}_l\right)\right]=0,\qquad i=1,2,\ldots,N_v.
\end{aligned}
\tag{9}
$$

$I_{ij}^{(k)}$ and $J_{ij}^{(k)}$ are obtained by implementing the Galerkin approach. For solving the ordinary differential equations described by Eq. (9), a continuation method is finally used. It should be noticed that in the present analysis, numerical calculations are performed using 16 shape functions. The present model captures the size influence via incorporating the scale parameter of the couple stress theory.

3 NUMERICAL RESULTS

For numerical results, the geometrical properties of the viscoelastic ultrasmall tube are taken as R_i=17.5 μm, R_o=25 μm, and L/R_o = 280. Moreover, the system material properties are assumed as v=0.38 and E=1.44 GPa,

ρ_t=1220 kg/m^3 and ρ_f =1000 kg/m^3 (Şimşek and Reddy 2013) in which ρ denotes the mass density; ''t'' and ''f'' denote the tube and fluid, respectively. These material properties are often employed for beams at microscale levels. The dimensionless parameters are γ =140, Γ =6.0, $\overline{c}_{vis}$ =0.0003, K_1=K_2=80, β=0.4406, $\overline{\mu}$ =0.4821, ϖ_f /ω_1=2 and Ξ_g =2.1047×10^5. Unless noted otherwise, the transverse deflection is plotted at α =0.45. The non-dimensional critical fluid velocity related to the divergence of the fluid-conveying ultrasmall tube is obtained as 8.4001.

The bifurcation plots of Poincaré sections of ultrasmall viscoelastic tubes containing pulsatile flowing fluid for a mean velocity a bit higher than the critical value (u_{f0}=8.5 > 8.4001) are plotted in Fig. 2. The ultrasmall system is in the supercritical regime. The first natural frequency of ultrasmall tubes containing pulsatile flowing fluid is obtained as ω_1= 5.29. From this figure, it can be concluded that the size-dependent nonlinear motion of the tube is of period-2 type for small values of u_{f1}. As the amplitude of the fluid velocity further increases, a wide range of distinct motion types such as period-1, period-2, period-6 and chaos is seen in the nonlinear complex vibrational response of the viscoelastic ultrasmall tube under longitudinal pretension. The first chaotic region starts at around u_{f1}=0.84, and the last one is around u_{f1}=2. To give more details, the Poincaré sections of the transverse motion for the system of Fig. 2 at u_{f1}=1.106 are plotted in Fig. 3. From this figure, it is seen that the type of the transverse motion for u_{f1}=1.106 is chaos. In addition, the size-dependent time history of the transverse motion for this case is illustrated in Fig. 4.

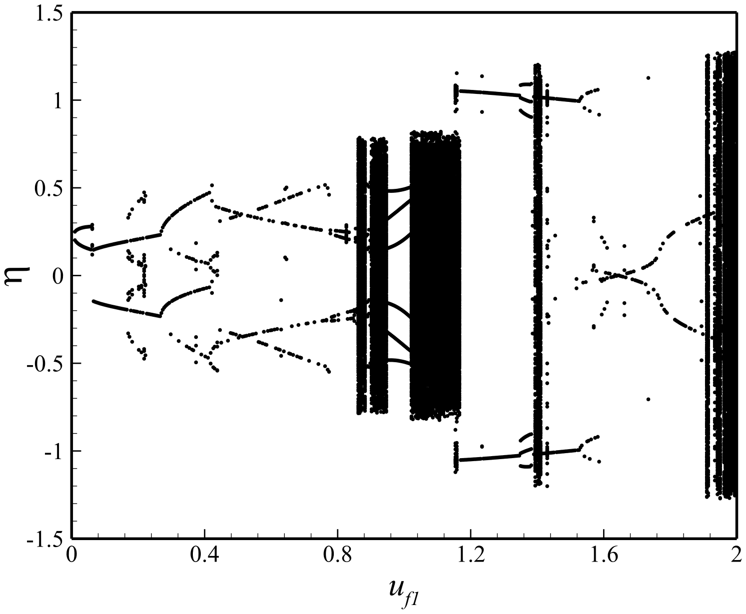

Figure 2: Bifurcation plots of ultrasmall viscoelastic tubes containing pulsatile flowing fluid for u_{f0}=8.5.

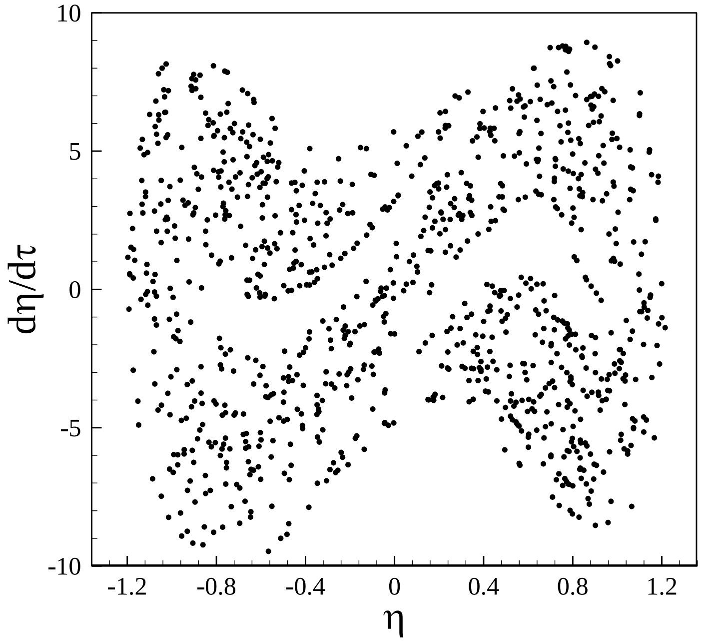

Figure 3: Poincaré sections of the transverse motion for the system chaos observed in Fig. 2 at u_{f1}=1.106.

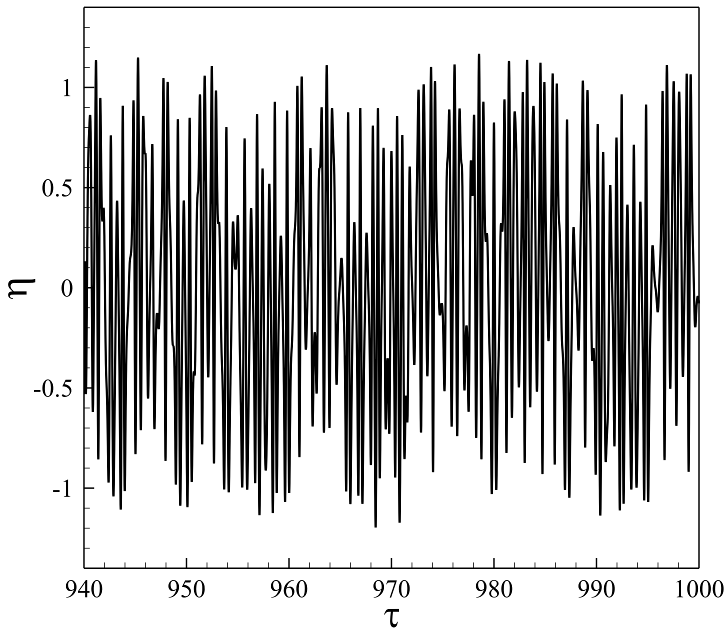

Figure 4: Time history of the transverse motion for the system chaos observed in Fig. 2 at u_{f1}=1.106.

4 CONCLUSIONS

The influence of the pulsation of the fluid flow on the complex vibrational behaviour of ultrasmall viscoelastic tubes surrounded by a nonlinear elastic medium was investigated. The emphasis was put on the chaos of the ultrasmall system. The MCST is employed for capturing the size influence on the vibrational behaviour. The influence of the internal friction was also incorporated by the Kelvin-Voigt model. The ultrasmall tube was under pretention along the axial direction. Employing an energy/work principle, the Galerkin approach and a continuation method, the governing equations were derived, discretised and solved. It was found that both the amplitude and mean value of the fluid velocity have a significant role in the complex vibrational response of ultrasmall viscoelastic tubes. In the super critical regime, various types of transverse motion are found depending on the value of the amplitude of the fluid flow. As a future work in this area to carry this research further, one can calibrate the scale parameter using molecular dynamics simulations or conducting experiments.

REFERENCES

Ansari, R, A Norouzzadeh, R Gholami, M Faghih Shojaei, and MA Darabi. 2016. "Geometrically nonlinear free vibration and instability of fluid-conveying nanoscale pipes including surface stress effects." Microfluidics and Nanofluidics 20 (1):28.

Aydogdu, Metin. 2015. "A nonlocal rod model for axial vibration of double-walled carbon nanotubes including axial van der Waals force effects." Journal of Vibration and Control 21 (16):3132-3154.

Bahaadini, R, and M Hosseini. 2016. "Nonlocal divergence and flutter instability analysis of embedded fluid-conveying carbon nanotube under magnetic field." Microfluidics and Nanofluidics 20 (7):108.

Cheaib, Farah, Gacia Kekejian, Sylvie Antoun, Mohammad Cheikh, and Issam Lakkis. 2016. "Microfluidic mixing using pulsating flows." Microfluidics and Nanofluidics 20 (5):70.

Dehrouyeh-Semnani, Amir Mehdi, Mansour Nikkhah-Bahrami, and Mohammad Reza Hairi Yazdi. 2017. "On nonlinear vibrations of micropipes conveying fluid." International Journal of Engineering Science 117:20-33.

Farajpour, MR, AR Shahidi, and A Farajpour. 2018. "A nonlocal continuum model for the biaxial buckling analysis of composite nanoplates with shape memory alloy nanowires." Materials Research Express 5 (3):035026.

Farajpour, MR, AR Shahidi, F Tabataba'i-Nasab, and A Farajpour. 2018. "Vibration of initially stressed carbon nanotubes under magneto-thermal environment for nanoparticle delivery via higher-order nonlocal strain gradient theory." The European Physical Journal Plus 133 (6):219.

Hadi, Amin, Mohammad Zamani Nejad, and Mohammad Hosseini. 2018. "Vibrations of three-dimensionally graded nanobeams." International Journal of Engineering Science 128:12-23.

Hosseini, Mohammad, and Reza Bahaadini. 2016. "Size dependent stability analysis of cantilever micro-pipes conveying fluid based on modified strain gradient theory." International Journal of Engineering Science 101:1-13.

Hosseini, Mohammad, Abbas Zandi Baghche Maryam, and Reza Bahaadini. 2017. "Forced vibrations of fluid-conveyed double piezoelectric functionally graded micropipes subjected to moving load." Microfluidics and Nanofluidics 21 (8):134.

Ke, Liao-Liang, Yue-Sheng Wang, Jie Yang, and Sritawat Kitipornchai. 2012. "Free vibration of size-dependent Mindlin microplates based on the modified couple stress theory." Journal of Sound and Vibration 331 (1):94-106.

Kural, Saim, and Erdoğan Özkaya. 2017. "Size-dependent vibrations of a micro beam conveying fluid and resting on an elastic foundation." Journal of Vibration and Control 23 (7):1106-1114.

Li, Li, Yujin Hu, Xiaobai Li, and Ling Ling. 2016. "Size-dependent effects on critical flow velocity of fluid-conveying microtubes via nonlocal strain gradient theory." Microfluidics and Nanofluidics 20 (5):76.

Liu, Hu, Zheng Lv, and Qi Li. 2017. "Flexural wave propagation in fluid-conveying carbon nanotubes with system uncertainties." Microfluidics and Nanofluidics 21 (8):140.

Murmu, T, S Adhikari, and CY Wang. 2011. "Torsional vibration of carbon nanotube–buckyball systems based on nonlocal elasticity theory." Physica E: Low-dimensional Systems and Nanostructures 43 (6):1276-1280.

Şimşek, M, and JN Reddy. 2013. "A unified higher order beam theory for buckling of a functionally graded microbeam embedded in elastic medium using modified couple stress theory." Composite Structures 101:47-58.

Şimşek, Mesut. 2010. "Dynamic analysis of an embedded microbeam carrying a moving microparticle based on the modified couple stress theory." International Journal of Engineering Science 48 (12):1721-1732.

Tang, Min, Qiao Ni, Lin Wang, Yangyang Luo, and Yikun Wang. 2014. "Nonlinear modeling and size-dependent vibration analysis of curved microtubes conveying fluid based on modified couple stress theory." International Journal of Engineering Science 84:1-10.

Wang, L. 2010. "Size-dependent vibration characteristics of fluid-conveying microtubes." Journal of Fluids and Structures 26 (4):675-684.

Warkiani, Majid Ebrahimi, Guofeng Guan, Khoo Bee Luan, Wong Cheng Lee, Ali Asgar S Bhagat, Parthiv Kant Chaudhuri, Daniel Shao-Weng Tan, Wan Teck Lim, Soo Chin Lee, and Peter CY Chen. 2014. "Slanted spiral microfluidics for the ultra-fast, label-free isolation of circulating tumor cells." Lab on a Chip 14 (1):128-137.